Nonlinear Dynamics **9**: 37–52, 1996.

An Energy Conserving Co-Rotational Procedure for Non-Linear Dynamics with Finite Elements

M. A. CRISFIELD and J. SHI
Department of Aeronautics, Imperial College, London, United Kingdom (FEA Professor) and Department of Aeronautics, Queen's University, Belfast, Northern Ireland

(Received: 7 September 1994; accepted: 29 September 1994)

Abstract. A new procedure is proposed for implicit dynamic analysis using the finite element method. The main aim is to give stable solutions with large time-steps in the presence of significant rigid body motions, in particular rotations. In contrast to most conventional approaches, the time integration strategy is closely linked to the "element technology" with the latter involving a form of co-rotational procedure. For the undamped situation, the solution procedure leads to an algorithm that exactly conserves energy when constant external forces are applied (i.e. with gravity loading).

Key words: Finite elements, time-integration, energy.

1. Introduction

Stewart [1] has highlighted the potential dangers of false solution from time-integration procedures with non-linear dynamics. For the finite element method, conventional procedures can be divided into two main types: explicit and implicit. The former is traditionally used for wave-propagation and high-velocity impact problems while the latter is more appropriate for structural applications dominated by the low frequency response although Downer *et al.* [2] have recently described an energy conserving explicit algorithm that gives excellent results for the latter problems. The present paper is devoted to implicit methods.

Conventional techniques adopt very similar predictor/corrector procedures to those used for non-linear statics. However, the out-of-balance force vector is now augmented by the mass-times-acceleration terms while the conventional static tangent stiffness matrix is augmented by a factor times the mass matrix if, as here, no damping is considered. Dynamic equilibrium is usually enforced at the end of the step.

Various time-integration strategies can be used for up-dating the velocities and accelerations with the Newmark methods [3–5] often being used. In the present paper, the average acceleration method (or trapezoidal rule with $\beta = 1/4$ and $\gamma = 1/2$) will be used to represent the "conventional procedure". The latter technique is "unconditionally stable" (irrespective of the time step) for *linear* problems. However, this stability does not extend to non-linear systems and consequently, as will be shown in the paper, the "conventional method" often requires absurdly small time steps if the solution is not to "lock" onto a higher energy state (see later). Attempts to overcome these difficulties have been made by both Haug *et al.* [7] and Hughes *et al.* [8] who used Lagrangian multipliers to enforce an energy constraint

In a standard algorithm, the time-integration procedure is totally divorced from the "element technology" (with the exception of the provision of the mass matrix). Most implicit dynamic procedures satisfy the dynamic equilibrium at the end of the step. More recently, Simo and co-workers have explored the idea of a "mid-point equilibrium" [9, 10] which follows on

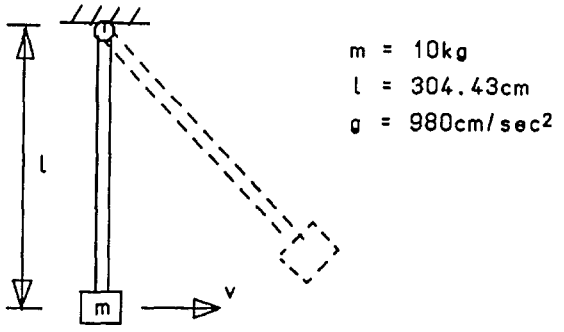

Fig. 1. Bathe's pendulum.

from the work of Hilber *et al.* [11] and Zienkiewicz *et al.* [12]. These concepts will be taken further in the present paper.

A key feature relates to the precise definition of the stresses and strains that are associated with the "mid-point" configuration. The present method relies heavily on co-rotational concepts [6, 13]. The latter have usually been used for statics with the key aim being to divorce the straining from the rigid body motions, in particular the rigid-body rotation. The authors have extended the ideas to dynamics [14, 15] and, to this end, have used both a mid-point configuration and "averaged strains". Similar ideas (although without the co-rotational framework) have recently been described by Simo and Tarnow [16, 17] in order to develop algorithms that conserve energy when constant external forces are applied.

In the first part of the paper, the theory is developed for simple two-dimensional truss elements and this is followed by a set of examples involving such elements. In the final part of the paper, the theory is described for the extension to two-dimensional beams and, in addition, ideas are outlined for the extension to three-dimensional beams and shells.

2. Motivation

The work was triggered by the authors' first attempts to apply dynamics to the simple pendulum shown in Figure 1 (with $EA = 10^{10}$ N). This problem has been discussed in detail by Bathe in his book [4] and study guide [18]. In both cases, the pendulum was dropped from the horizontal position, while in the present analysis, it is "fired" with an initial horizontal velocity of 772.5 cm/sec from the vertical position. The basic behaviour is similar.

From the response in Figure 2, one can see that although the period is of the order of 4.0 seconds "conventional procedures" (as previously defined) require a time step of the order of 0.025 seconds to give a satisfactory solution.

Figure 2 shows that if a time step of 0.1 seconds is adopted, the solution "locks" at a position close to the initial position after one and a quarter periods. Figure 3 shows that, prior to this "locking", there has been a build-up of energy with an increasing percentage going into strain energy associated with an oscillating axial strain (Figure 4). This phenomenon was earlier noted by Bathe [18]. The term "locking" is used because, although the bar still moves, the overall (lower mode) motions are now fairly small while the local axial stretching (higher mode) dominates.

It would be possible to overcome these difficulties for this simple pendulum by switching variables to use the rotation and stretch. However, the procedure could not then be easily extended to other configurations within a conventional finite element framework. Before

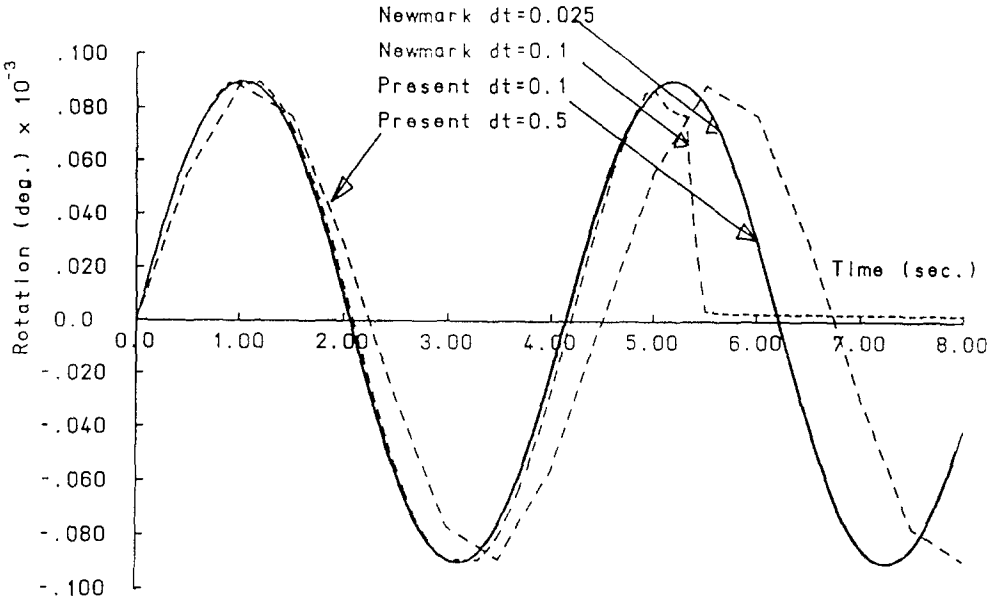

Fig. 2. Relationships between rotation and time for Bathe's pendulum.

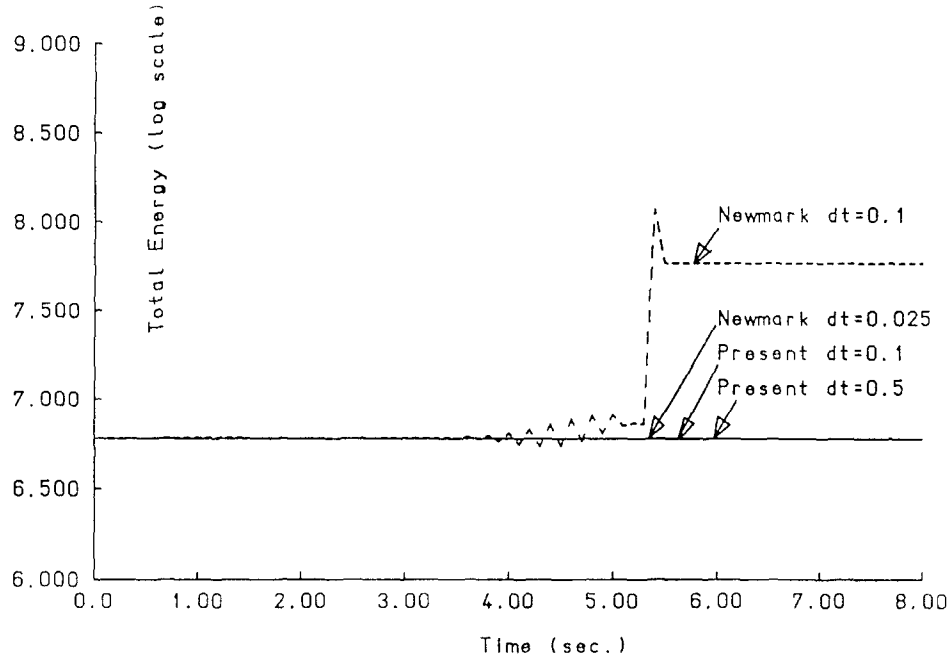

Fig. 3. Relationships between energy and time for Bathe's pendulum.

detailing the theory for the new method, we note that, for this problem, it leads to a very satisfactory solution with a time step of 0.1 (Figures 2 and 3) and that even with a time step of 0.5, no locking is encountered (Figures 2 and 3).

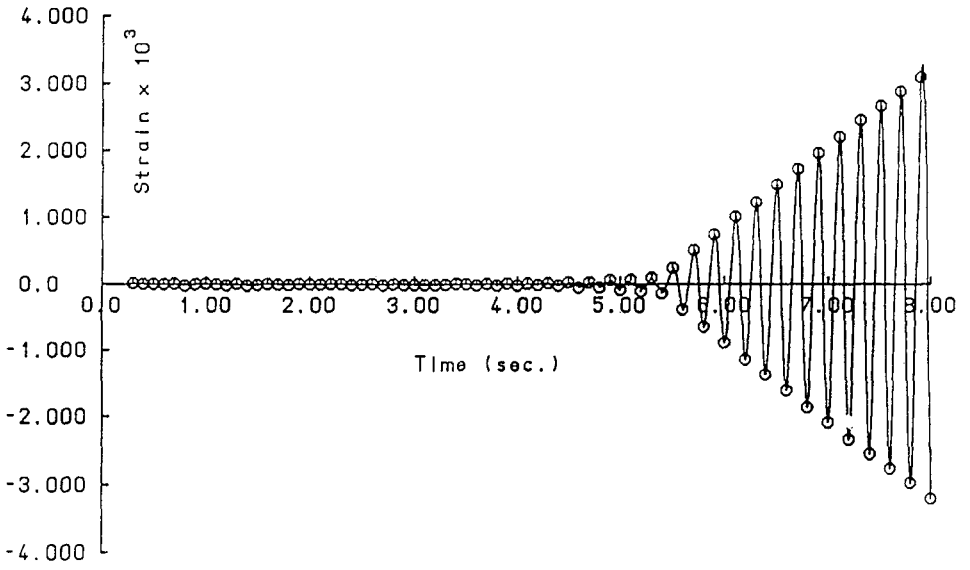

Fig. 4. Relationships between axial strain and time for Bathe's pendulum.

3. Theory

Before describing the new method, a brief description is given of the "conventional" trapezoidal rule (or average acceleration method). The displacements, $\mathbf{d}$, are chosen as the "driving variables" so that the velocity at the end of the step, $\mathbf{v}_{n+1}$, can be obtained via

$$\mathbf{v}_{n+1} = \frac{2}{\Delta t}(\mathbf{d}_{n+1} - \mathbf{d}_n) - \mathbf{v}_n = \frac{2}{\Delta t}\Delta\mathbf{d} - \mathbf{v}_n \tag{1}$$

while the acceleration is then obtained from

$$\mathbf{a}_{n+1} = \frac{2}{\Delta t}(\mathbf{v}_{n+1} - \mathbf{v}_n) - \mathbf{a}_n = \frac{2}{\Delta t}\Delta\mathbf{v} - \mathbf{a}_n. \tag{2}$$

Without damping, the equilibrium equations at the end of the step are given by

$$\mathbf{g}_{n+1} = \mathbf{q}_{i,n+1} + \mathbf{M}\mathbf{a}_{n+1} - \mathbf{q}_{e,n+1} = 0, \tag{3}$$

where $\mathbf{q}_i$ are the (static) internal forces, $\mathbf{M}$ is the mass matrix and $\mathbf{q}_e$ are the external forces. Equations (3) may be solved using the Newton–Raphson method in which the linearisation of (3) is used to obtain the effective tangent stiffness matrix.

In the following, we will concentrate on the equations for a simple two noded truss element as shown in Figure 5. The external forces and the masses will be assumed fixed and related to the element thereby allowing us to concentrate on the latter. In these circumstances, with the co-rotational approach [6], equations (3) become

$$\mathbf{g}_{n+1} = N_{n+1}\begin{pmatrix} -\mathbf{e}_{n+1} \\ \mathbf{e}_{n+1} \end{pmatrix} + \frac{2}{\Delta t}\begin{pmatrix} m_1\Delta\mathbf{v}_1 \\ m_2\Delta\mathbf{v}_2 \end{pmatrix} - \begin{pmatrix} m_1\mathbf{a}_1 \\ m_2\mathbf{a}_2 \end{pmatrix}_n - \begin{pmatrix} \mathbf{q}_{e1} \\ \mathbf{q}_{e2} \end{pmatrix} = 0, \tag{4}$$

where N_{n+1} is the axial force (tensile positive) in the bar at the end of the step and $\mathbf{e}_{n+1}$ is the unit vector lying along the bar (Figure 5).

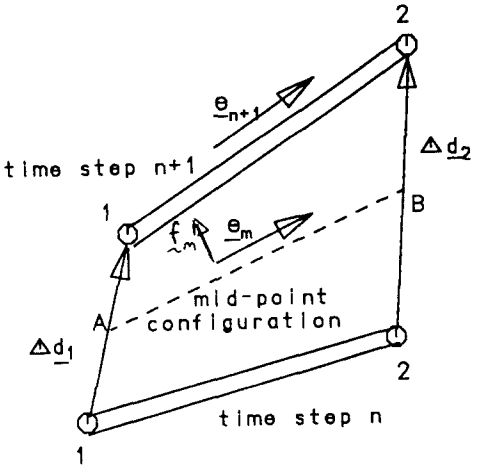

Fig. 5. Two-noded truss element.

In [9], Simo and co-workers have proposed a "mid-point procedure" in which, for the up-dating, equation (1) is retained but equation (2), which can be re-expressed as

$$\mathbf{a}_{\text{av}} = \frac{1}{\Delta t}\,\Delta\mathbf{v}, \tag{5}$$

is replaced by

$$\mathbf{a}_m = \frac{1}{\Delta t}\,\Delta\mathbf{v} \tag{6}$$

with the end-point equilibrium of (3) being replaced by the mid-point equilibrium of

$$\mathbf{g}_m = \mathbf{q}_{i,m} + \mathbf{M}\mathbf{a}_m - \mathbf{q}_{e,m} = 0. \tag{7}$$

With the previous assumptions, for the bar element of Figure 5, this leads, in place of (4) to

$$\mathbf{g}_m = N_m \begin{pmatrix} -\mathbf{e}_m \\ \mathbf{e}_m \end{pmatrix} + \frac{1}{\Delta t}\begin{pmatrix} m_1\Delta\mathbf{v}_1 \\ m_2\Delta\mathbf{v}_2 \end{pmatrix} - \begin{pmatrix} \mathbf{q}_{e1} \\ \mathbf{q}_{e2} \end{pmatrix} = 0. \tag{8}$$

The key factor involves the definition of N_m via its associated strain. In [9], Simo and co-workers obtained the mid-point strain directly from the mid-point configuration. However, as illustrated in Figure 6, for the previous pendulum problem, this leads to high artificial straining. In order to remove the artificial straining, in [14, 15], the authors simply redefined N_m as a factor β (which will be defined later) times the average of the axial forces at the beginning and ends of the step, i.e.,

$$N_m = \beta(N_n + N_{n+1})/2 = \beta N_{\text{av}}. \tag{9}$$

Simo and Tarnow [16, 17] have adopted a similar approach (although without the factor β for reasons that will be discussed later).

To complete the definition of the terms in (8), the force in the bar at the current configuration is obtained via

$$N_{n+1} = N_{\text{init}} + \frac{EA}{\ell_o}\,(\ell_{n+1} - \ell_o), \tag{10}$$

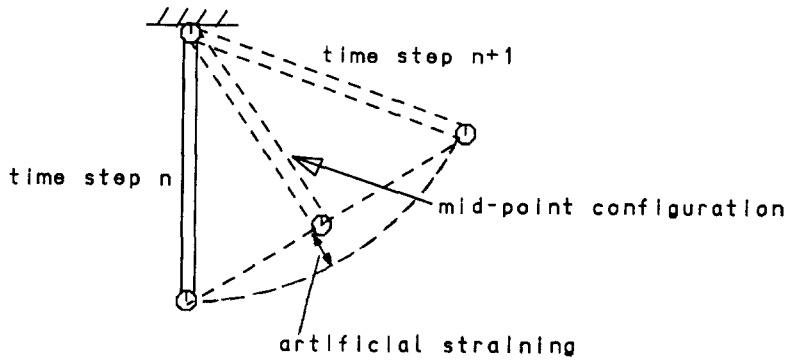

Fig. 6. Artificial straining with conventional mid-point procedure.

with ℓ_0 as the initial length of the bar. The current length is simply obtained using

$$\ell_{n+1}^2 = \mathbf{x}_{21,n+1}^T \mathbf{x}_{21,n+1} = (\mathbf{X}_{21} + \mathbf{d}_{21})^T (\mathbf{X}_{21} + \mathbf{d}_{21}), \tag{11}$$

where, for example $\mathbf{d}_{21} = \mathbf{d}_2 - \mathbf{d}_1$ and $\mathbf{X}_1$ and $\mathbf{X}_2$ are the initial position vectors of nodes 1 and 2. In addition, the mid-point unit vector, $\mathbf{e}_m$ in (8) is obtained as

$$\mathbf{e}_m = \left(\mathbf{x}_{21,n} + \frac{1}{2} \Delta \mathbf{d}_{21} \right) / \ell_{\text{mt}}, \tag{12}$$

where the true mid-point length, ℓ_{mt} (between points A and B in Figure 5) is given by

$$\ell_{\text{mt}} = \left\| \mathbf{x}_{21,n} + \frac{1}{2} \Delta \mathbf{d}_{21} \right\|. \tag{13}$$

(The procedure breaks down if the incremental rotation is 180° when ℓ_{mt} becomes zero if there is no stretching. Such enormous increments are unlikely to be used.) The factor β in (9) is provided to ensure energy conservation.

Using (1) the change in kinetic energy at a node can be obtained as

$$\Delta K = \frac{1}{2} m(\mathbf{v}_{n+1}^T \mathbf{v}_{n+1} - \mathbf{v}_n^T \mathbf{v}_n) = m \mathbf{v}_{\text{av}}^T \Delta \mathbf{v} = \frac{1}{\Delta t} m \Delta \mathbf{v}^T \Delta \mathbf{d}, \tag{14}$$

while with the previous assumptions, the change in external potential energy at a node is

$$\Delta P = -\mathbf{q}_e^T \Delta \mathbf{d}. \tag{15}$$

For an element, the change in strain energy is given by

$$\Delta \varphi = \frac{\ell_o}{2EA} (N_{n+1}^2 - N_n^2) = \frac{\ell_o}{EA} N_{\text{av}} \Delta N, \tag{16}$$

where

$$\Delta N = \frac{EA}{\ell_o} (\ell_{n+1} - \ell_n) = \frac{EA}{\ell_o} \frac{(\ell_{n+1}^2 - \ell_n^2)}{(\ell_{n+1} + \ell_n)}, \tag{17}$$

while

$$\ell_{n+1}^2 - \ell_n^2 = 2\mathbf{x}_{21,n}^T \Delta \mathbf{d}_{21} + \Delta \mathbf{d}_{21}^T \Delta \mathbf{d}_{21} = 2\ell_{\text{mt}} \mathbf{e}_m^T \Delta \mathbf{d}_{21}, \tag{18}$$

with $\ell_{\rm mt}$ having been previously defined in (13). From (16)–(18), we obtain

$$\Delta\varphi = \beta N_{\rm av}\mathbf{e}_m^T\Delta\mathbf{d}_{21}, \tag{19}$$

with

$$\beta = \frac{\ell_{\rm mt}}{\ell_{\rm mav}} = \frac{2\ell_{\rm mt}}{(\ell_n + \ell_{n+1})}. \tag{20}$$

Hence, with the mid-point axial force being given by (9) with β from (20), the total energy chance, can be expressed as

$$\Delta\phi = \Delta\varphi + \Delta K + \Delta P = \mathbf{g}^T\begin{pmatrix}\Delta\mathbf{d}_1\\ \Delta\mathbf{d}_2\end{pmatrix}, \tag{21}$$

with $\mathbf{g}$ from (8). At equilibrium $\mathbf{g}$ is zero and hence, at equilibrium, energy is exactly preserved. It is worth noting that the factor β tends to unity as the step-size tends to zero and is also unity when there is no rotation.

Equations (7)–(9) can be linearised to give

$$\delta\mathbf{g}_m = \delta\mathbf{q}_{i,m} + \frac{1}{\Delta t}\begin{pmatrix}m_1\delta\mathbf{v}_1\\ m_2\delta\mathbf{v}_2\end{pmatrix} = \bar{\mathbf{K}}_t\delta\mathbf{d}, \tag{22}$$

where, via (1),

$$\bar{\mathbf{K}}_t = \mathbf{K}_t + \frac{2}{\Delta t^2}\begin{bmatrix}m_1\mathbf{I} & 0\\ 0 & m_2\mathbf{I}\end{bmatrix} \tag{23}$$

and

$$\delta\mathbf{q}_{i,m} = \delta N_m\begin{pmatrix}-\mathbf{e}_m\\ \mathbf{e}_m\end{pmatrix} + N_m\begin{pmatrix}-\delta\mathbf{e}_m\\ \delta\mathbf{e}_m\end{pmatrix} = \mathbf{K}_t\delta\mathbf{d}. \tag{24}$$

Full details are given in [14]. It should be noted that $\mathbf{K}_t$ is non-symmetric although an artificial symmetrisation can be applied if the time steps are not too large [14].

3.1. An Alternative Formulation

Following on from the work in [16], Simo and Tarnow [17] have very recently proposed an energy preserving procedure for shells. We will now attempt to establish links with the present formulation.

If a total Lagrangian formulation is adopted, equation (4) becomes [6]

$$\mathbf{g}_{n+1} = N_{n+1}\mathbf{b}_{n+1} + \frac{1}{\Delta t}\begin{pmatrix}m_1\Delta\mathbf{v}_1\\ m_2\Delta\mathbf{v}_2\end{pmatrix} - \begin{pmatrix}m_1\mathbf{a}_1\\ m_2\mathbf{a}_2\end{pmatrix}_n - \begin{pmatrix}\mathbf{q}_{e1}\\ \mathbf{q}_{e2}\end{pmatrix} = \mathbf{0}, \tag{25}$$

where

$$\mathbf{b}_{n+1} = \frac{\ell_{n+1}}{\ell_o}\begin{pmatrix}-\mathbf{e}_{n+1}\\ \mathbf{e}_{n+1}\end{pmatrix} \tag{26}$$

and in place of (10):

$$N_{n+1} = N_{\text{init}} + \frac{EA}{2\ell_o^2}(\ell_{n+1}^2 - \ell_o^2). \tag{27}$$

Applying the approach of Simo and Tarnow [17], in place of (8), the mid-point equilibrium would take the form

$$\mathbf{g}_m = N_{\text{av}}\frac{1}{2}(\mathbf{b}_n + \mathbf{b}_{n+1}) + \frac{1}{\Delta t}\begin{pmatrix} m_1\Delta\mathbf{v}_1 \\ m_2\Delta\mathbf{v}_2 \end{pmatrix} - \begin{pmatrix} \mathbf{q}_{e1} \\ \mathbf{q}_{e2} \end{pmatrix} = \mathbf{0}, \tag{28}$$

where N_{av} is simply the mean of the N's at configurations n and $n+1$ (as before but with (27) now defining the N's). Following the lines adopted previously, it is easy to show that this approach leads to an energy conserving algorithm. It can also be shown that, provided the strains (but not the deformations or rotations) are small, we can adopt equation (28) for the present co-rotational formulation with the N's being given by (10) and that this leads to a procedure that is very close to that given previously. By comparing (28) with (8) and (9), it is clear that we merely need to establish that

$$\frac{1}{2}(\mathbf{b}_n + \mathbf{b}_{n+1}) = \frac{1}{2}\left(\begin{pmatrix} -\mathbf{e}_n \\ \mathbf{e}_n \end{pmatrix} + \begin{pmatrix} -\mathbf{e}_{n+1} \\ \mathbf{e}_{n+1} \end{pmatrix}\right) \simeq \frac{\ell_{\text{mt}}}{\ell_{\text{mav}}}\begin{pmatrix} -\mathbf{e}_m \\ \mathbf{e}_m \end{pmatrix} = \beta\begin{pmatrix} -\mathbf{e}_m \\ \mathbf{e}_m \end{pmatrix}, \tag{29}$$

where we are now using the co-rotational form for the **b** vector (see (4) and [6]). With small strains, it is easy to establish that this relationship does indeed hold because

$$\begin{aligned} \frac{1}{2}(\mathbf{e}_n + \mathbf{e}_{n+1}) &= \frac{\ell_n + \ell_{n+1}}{2\ell_n\ell_{n+1}}\left(\mathbf{x}_{21,n} + \frac{\ell_n}{\ell_n + \ell_{n+1}}\Delta\mathbf{d}_{21}\right) \\ &\simeq \frac{1}{\ell_{\text{mav}}}\left(\mathbf{x}_{21,n} + \frac{1}{2}\Delta\mathbf{d}_{21}\right) = \frac{\ell_{\text{mt}}}{\ell_{\text{mav}}}\mathbf{e}_m = \beta\mathbf{e}_m. \end{aligned} \tag{30}$$

4. Numerical Examples

The following examples have been computed using the original formulation [14, 15] rather than the previous "alternative formulation". For the first set of examples which involve small strains, we would expect almost identical solutions via the "alternative formulation".

The numerical results for Bathe's pendulum have already been described. In the first set of following examples, Young's modulus times the area had been chosen to be 10^{10} N so that the bars or chain-links are nearly rigid. In all cases, fixed time increments have been employed. The terminology "Newmark" refers to the Newmark scheme with $\beta = 0.25$ and $\gamma = 0.5$.

4.1. Four-Chain System

Figure 7 shows the computed response for a four-bar chain of the same EA value as the previous pendulum and of total length 400 which is free to fly (in the absence of gravity). The chain was given an initial linearly varying downward velocity which was zero at the right-hand end and was equivalent to a rotation about the right-hand end of 1 rad/sec. The density was taken as 1 Kg/m.

The response for the present method involves the chain remaining straight as it should. In contrast the Newmark method (with $\beta = 1/4, \gamma = 1/2$) starts by giving a sensible solution but

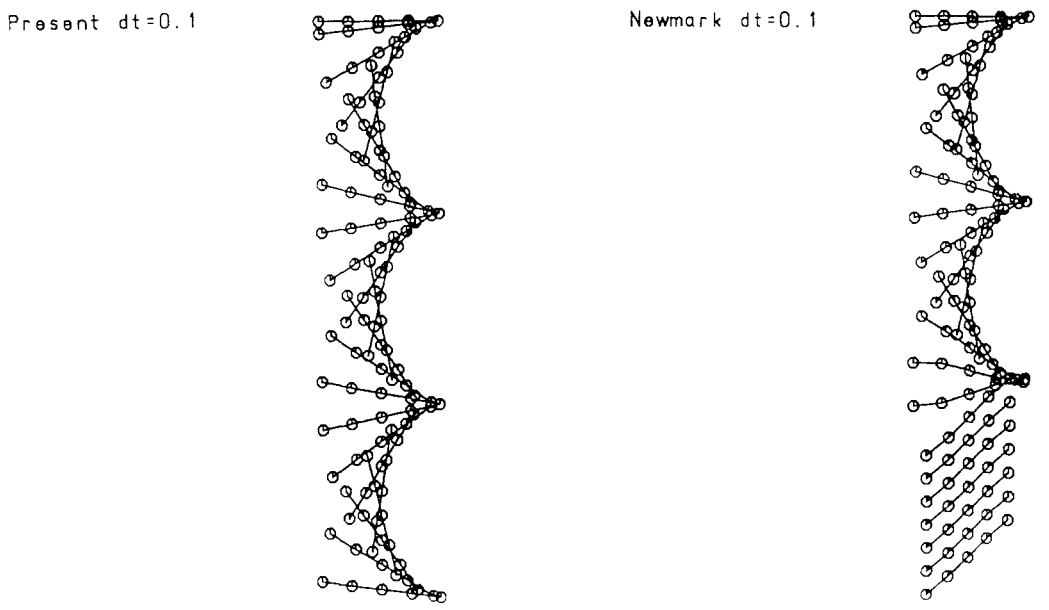

Fig. 7. Deformed configurations for free-flying four-bar chain.

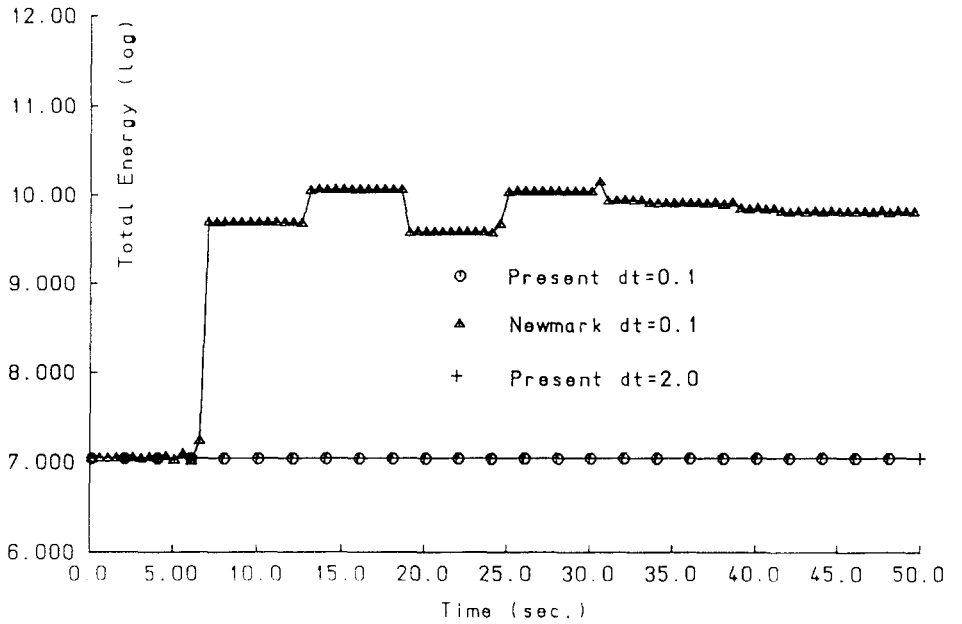

Fig. 8. Relationships between energy and time for free-flying four-bar chain.

suddenly jumps to a false energy configuration (Figure 8) associated with axial oscillation of the bar and no overall rotation (Figure 7)! The solutions in Figure 7 are related to a fixed time increment of 0.1 seconds. They are compared with the exact solution for the horizontal tip-displacement at the left-hand end in Figure 9. The "exact" solution is computed by assuming that the bars are rigid. It can be seen that the present method leads to an effectively exact solution with $\Delta t = 0.1$ while even with $\Delta t = 2.0$, although there is some period elongation,

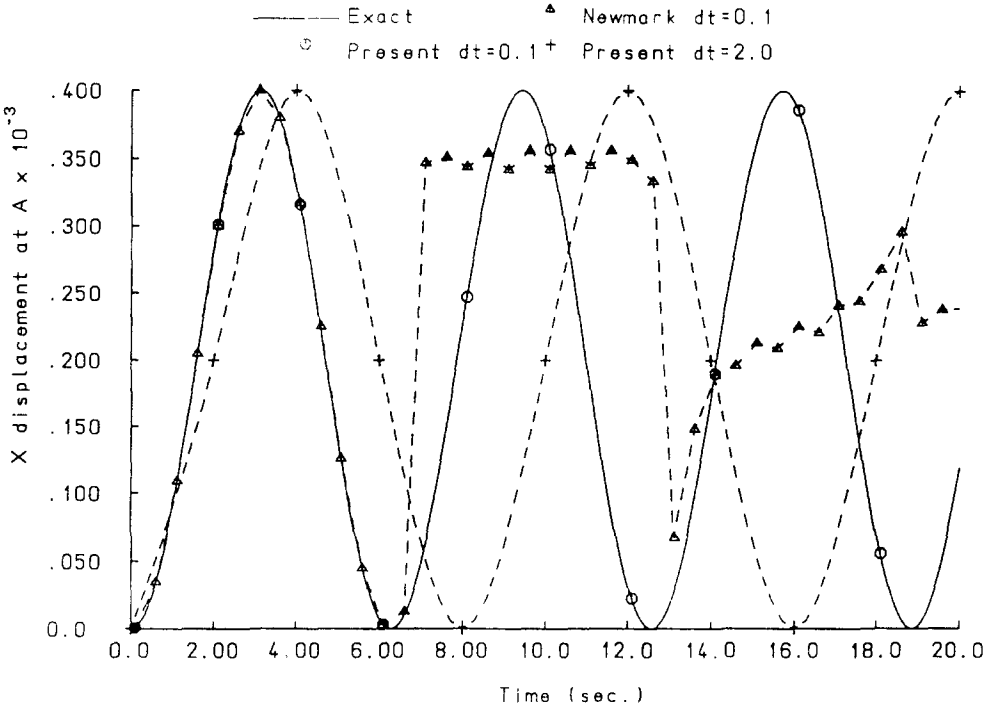

Fig. 9. Relationships between tip-displacement and time for free-flying four-bar chain.

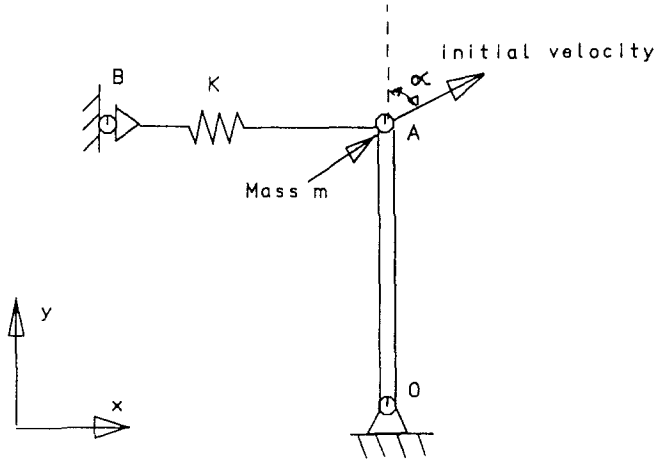

Fig. 10. Simple model with two degrees-of-freedom.

no "locking" occurs. The present method not only conserves energy (Figure 8) but also angular momentum [14].

4.2. Simple Model with Two Degrees-of-Freedom

The first author and co-worker have described [19, 20] an energy framework for the simple model problem shown in Figure 10. The bar OA is modelled with one of the truss elements discussed previously while in the x-direction a linear spring of stiffness K is provided (AB being forced to remain horizontal). The point mass, m, was set to unity, the initial length, ℓ_o,

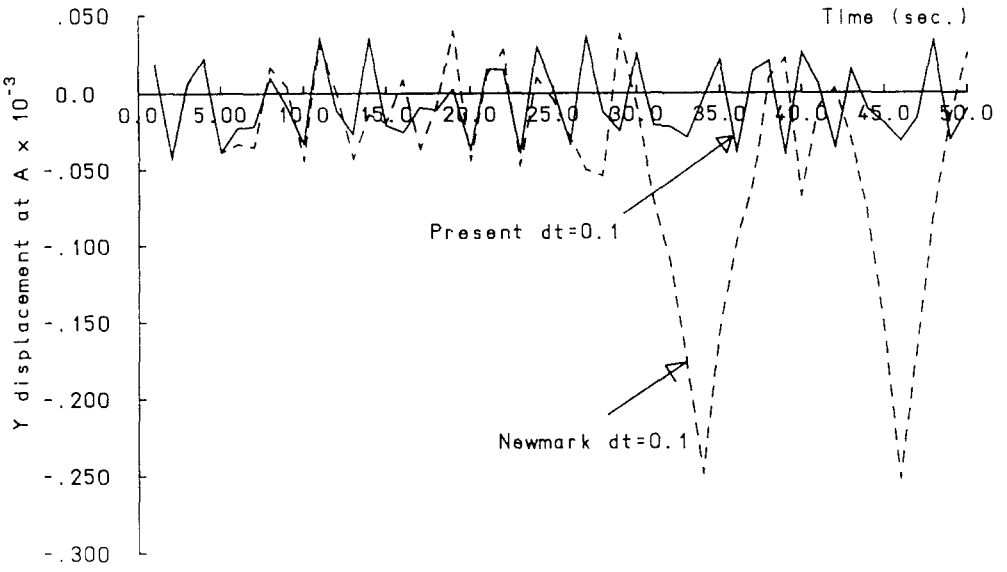

Fig. 11. Relationships between vertical displacement (y) and time for simple model.

to 100 and Young's modulus times the area of the bar OA was set to 500 so that the stiffness of the bar was 5.0 which is five times larger than the stiffness provided for the linear spring, BA, for which $K = 1$. No gravity effects were considered.

The energy framework can be used to show that if the initial non-dimensional kinetic energy, $\bar{T} = 2T/(K\ell_o^2)$, is greater than the critical value $\bar{T}_{cr} = 0.833$, the system *may*, within a certain time period, "escape" from a response associated with a low amplitude so as to respond with a "large amplitude". However, if $\bar{T} < \bar{T}_{cr}$, such "escaping motion" should be impossible. For the present study, $\bar{T}$ has been set to 0.8 with the angle α in Figure 10 being 135°.

Figure 11 shows the computed relationships between the vertical displacement (y-direction – Figure 10) and time. As anticipated, with the present method, the motion does not "escape" (Figures 11 and 12a). In contrast, with the "Newmark method", escape occurs after about 30 seconds (Figures 11 and 12b). The latter, false response, is very similar to the true response which might have been obtained with an initial kinetic energy, $\bar{T} > \bar{T}_{cr}$ (see [19, 20]).

5. Extensions to Other Types of Element

The extension of the previous formulation to cover three-dimensional truss elements is trivial. Indeed the basic equations remain unaltered. In the following, we will initially outline a possible extension to cover two-dimensional beams.

The equivalent static formulation is detailed by the author in [6] and is closely related to the work of Oran [21]. It is based on a Kirchhoff beam formulation without shear deformation although an equivalent formulation based on Timoshenko theory can easily be derived [6]. In relation to Figure 5, we again have two nodes but now with a rotational variable, θ, added to the two translational variables, $\mathbf{d}$ at each node. Collectively the structural "displacements" are then

$$\mathbf{p}^T = (\mathbf{d}_1^T, \theta_1, \mathbf{d}_2, \theta_2). \tag{31}$$

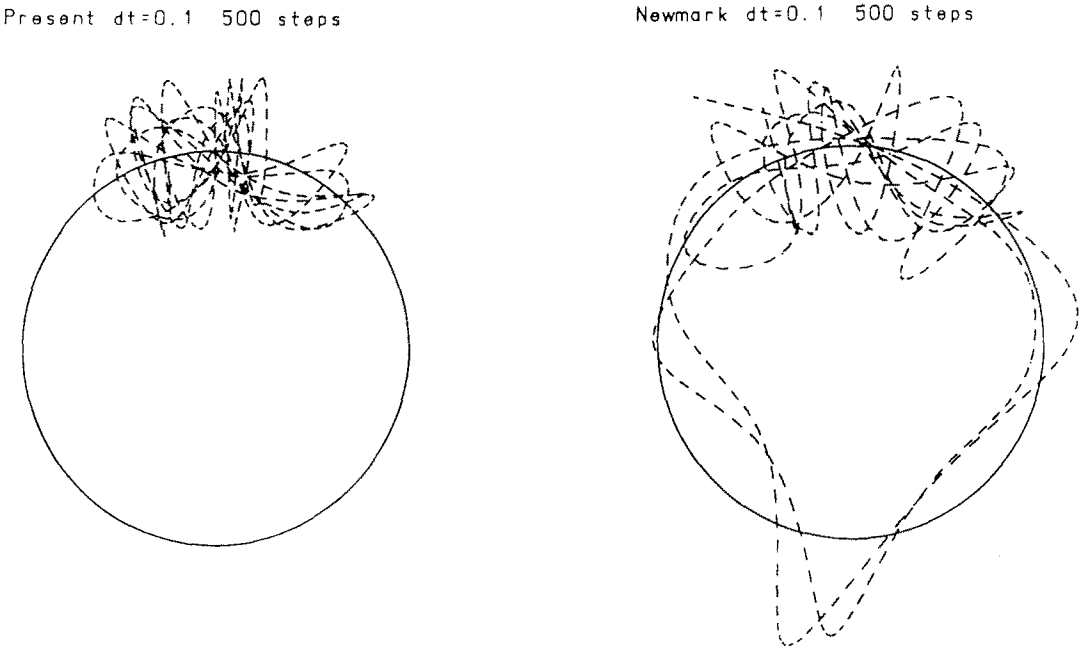

Fig. 12. Traces of motion of point A for simple model. (a) Present solution and (b) solution via "Newmark".

For the bending deformations, we require two local rotations,

$$\theta_{\ell 1} = \theta_1 - \alpha; \qquad \theta_{\ell 2} = \theta_2 - \alpha, \tag{32}$$

where α is the rigid body rotation which at configuration $n+1$ can be computed from

$$\sin\alpha = \frac{1}{\ell_o \ell_{n+1}} \mathbf{x}_{21,o} \times \mathbf{x}_{21,n+1}, \tag{33}$$

where the lengths ℓ_o (initial) and ℓ_{n+1} (current) follow the same equations as used for the truss element (see (11)). It should be noted that the curved length component is neglected in this basic formulation. It is perfectly possible to add additional terms to allow for these effects [6] via rotating "shallow arch terms".

The local bending moments, $\bar{M}_1$ and $\bar{M}_2$ are computed from the local θ's via

$$\begin{pmatrix} \bar{M}_1 \\ \bar{M}_2 \end{pmatrix} = \frac{EI}{\ell_o} \begin{bmatrix} 4 & 2 \\ 2 & 4 \end{bmatrix} \begin{pmatrix} \theta_{\ell 1} \\ \theta_{\ell 2} \end{pmatrix}. \tag{34}$$

In relation to the following dynamic formulation, we require a good approximation to (33) that is valid for the change of rigid body rotation between configurations n and $n+1$. Such an approximation follows from Figure 13 and is given by

$$\Delta\alpha = \frac{1}{2}\left(\frac{1}{\ell_n}\mathbf{f}_n + \frac{1}{\ell_{n+1}}\mathbf{f}_{n+1}\right)^T \Delta\mathbf{d}_{21}. \tag{35}$$

Equation (35) effectively replaces $\Delta\alpha$ with $\sin\Delta\alpha$ if the axial strains are small.

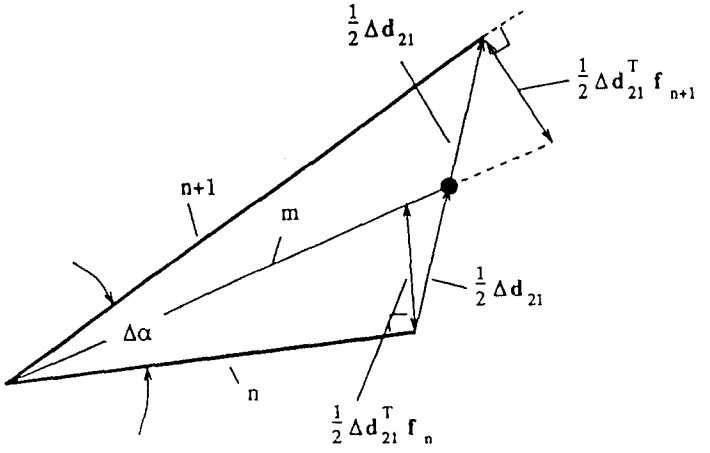

Fig. 13. computation of the rigid-body rotation.

The axial energy for the beam element follows identically that given previously for the truss and hence we will concentrate on the bending energy. For the latter, the static internal force vector is given by [6]:

$$\mathbf{q}_{i,n+1} = \mathbf{B}_{n+1}^T \begin{pmatrix} \bar{M}_1 \\ \bar{M}_2 \end{pmatrix}, \tag{36}$$

where the "**B** matrix" is given by

$$\mathbf{B}_{n+1}^T = \left[\frac{1}{\ell_{n+1}} \begin{pmatrix} \mathbf{f}_{n+1} \\ \ell_{n+1} \\ -\mathbf{f}_{n+1} \\ 0 \end{pmatrix}, \frac{1}{\ell_{n+1}} \begin{pmatrix} \mathbf{f}_{n+1} \\ 0 \\ -\mathbf{f}_{n+1} \\ \ell_{n+1} \end{pmatrix} \right], \tag{37}$$

and the unit vector $\mathbf{f}_{n+1}$ is orthogonal to $\mathbf{e}_{n+1}$ in the same manner that $\mathbf{f}_m$ is orthogonal to $\mathbf{e}_m$ (see Figure 5). If we now adopt the average **B** matrix approach of Simo and Tarnow, we arrive at the following mid-point dynamic equilibrium equations:

$$\begin{aligned} \mathbf{g}_m &= N_{\text{av}} \frac{1}{2} (\mathbf{b}_n + \mathbf{b}_{n+1}) + \frac{1}{2} (\mathbf{B}_n + \mathbf{B}_{n+1})^T \begin{pmatrix} \bar{M}_{\text{av},1} \\ \bar{M}_{\text{av},2} \end{pmatrix} \\ &\quad + \frac{1}{\Delta t} \begin{pmatrix} m_1 \Delta \mathbf{v}_1 \\ \bar{m}_1 \Delta \dot{\theta}_1 \\ m_2 \Delta \mathbf{v}_2 \\ \bar{m}_2 \Delta \dot{\theta}_2 \end{pmatrix} - \mathbf{q}_{e,m} = 0, \end{aligned} \tag{38}$$

where we have also adopted the average **B** matrix approach for the axial part (see Section 3.1) so that the **b** vectors would be as given in (29). The $\bar{m}$ terms in (38) involve the "lumped" rotational mass while the term $\bar{M}_{\text{av},1}$ is simply the average of the $\bar{M}$ values from configurations n and $n+1$ (following N_{av} – see (16)).

The time integration of the rotational variables follows the same form as that adopted for the translations, i.e.,

$$\dot{\theta}_{n+1} = \frac{2}{\Delta t} \Delta\theta - \dot{\theta}_n \tag{39}$$

$$\ddot{\theta}_m = \frac{1}{\Delta t}\,\Delta\dot{\theta}. \tag{40}$$

To consider the energy conservation, we firstly supplement the axial strain energy of (19) with the bending strain energy

$$\begin{aligned}\Delta\varphi_b &= \bar{M}_{\mathrm{av},1}\Delta\theta_{\ell 1} + \bar{M}_{\mathrm{av},2}\Delta\theta_{\ell 2}\\ &= \bar{M}_{\mathrm{av},1}(\Delta\theta_1 - \Delta\alpha) + \bar{M}_{\mathrm{av},2}(\Delta\theta_2 - \Delta\alpha),\end{aligned} \tag{41}$$

where (purely for this energy calculation) the rigid rotation $\Delta\alpha$ is given by (35). In addition, for any node, we have a contribution to the kinetic energy of

$$\Delta T_b = \frac{1}{2}\,\bar{m}(\dot{\theta}_n + \dot{\theta}_{n+1})\Delta\dot{\theta} = \frac{\bar{m}}{2\Delta t}\,\Delta\dot{\theta}\Delta\theta, \tag{42}$$

where we have used (39). Combining (41), (42) and (35) with (14), (15) and (19) leads to the relationship

$$\Delta\phi = \Delta\varphi + \Delta T + \Delta P = \mathbf{g}_m^T\Delta\mathbf{p}, \tag{43}$$

where $\mathbf{g}_m$ is the residual term given by (38) and $\Delta\mathbf{p}$ contains the incremental nodal "displacements". As with the truss formulation the change of energy in (43) will therefore be zero once we have iterated to the state where the residual in (38) is zero.

In contrast to the truss element formulation, this observation is only valid for the beam with moderate sized rotation increments for which (35) is a reasonable approximation. (Note that we use (33) – in incremental form – rather than (35) in computing the bending moments from (34).) Since the original draft of this paper, we have shown numerically that the proposed formulation for beams gives significantly better solutions than does the standard Newmark algorithm. Work is in hand to modify the procedure with a view to obtaining full energy conservation irrespective of the size of the rigid rotation increment. In our current formulation, in which the main features are essentially the same as those just described, we have adopted a slightly different form for the co-rotational approach in which the co-rotational aspects are kept totally separate from the conventional linear formulation which is applied at the local level [23]. Hence, with a conventional end-point equilibrium, the static part of the internal force vector would be written as

$$\mathbf{q}_{i,n+1} = \mathbf{T}_{n+1}\mathbf{q}_{\ell i,n+1}, \tag{44}$$

where $\mathbf{q}_{\ell i,n+1}$ is the local internal force vector computed by using a standard linear element stiffness matrix in relation to the local system [6, 23] and $\mathbf{T}_{n+1}$ is the transformation matrix at step $n+1$ whereby

$$\delta\mathbf{p}_\ell = \mathbf{T}\delta\mathbf{p}, \tag{45}$$

with $\delta\mathbf{p}_\ell$ as the small change in local nodal "displacements" and $\delta\mathbf{p}$ as the small change in global nodal "displacements" (all at configuration $n+1$). For the present "mid-point" formulation, we compute the static part of the mid-point internal force vector via

$$\mathbf{q}_{i,m} = \left[\frac{\mathbf{T}_n + \mathbf{T}_{n+1}}{2}\right]^T\left(\frac{\mathbf{q}_{i\ell,n} + \mathbf{q}_{i\ell,n+1}}{2}\right). \tag{46}$$

In relation to static analysis, the author has extended the two-dimensional co-rotational formulation to three-dimensional beams [22] and, in future work, it is intended to apply a similar approach to the dynamic case. The extension to dynamics will also be applied to a simple co-rotational triangular shell element [13]. If the formulation is restricted to small strains (although with large deformations and rotations), the simplest approach would be to adopt the method based on the average **B** matrix (or transformation matrix **T** as indicated above). For the shell element of [13], which has only one rotational variable per each mid-side, the resulting formulation should be very simple.

6. Conclusions

An energy conserving time-integration procedure has been devised that is based on the co-rotational approach and involves a mid-point configuration in conjunction with averaged strains. Examples have been presented showing the application of the technique to simple two-dimensional truss elements. It has been shown that "conventional techniques" lead to solutions that may suddenly jump to higher energy states that are associated with high frequency axial oscillations. Alternatively, they may exhibit false "escaping motion" that should be associated with a structure subject to a higher initial kinetic energy. In contrast, the current solutions remain stable with large time-steps.

A disadvantage of the method is that it involves a non-symmetric effective tangent stiffness matrix. However, this disadvantage should be more than compensated by the stability of the method. In addition, it is possible to artificially symmetrise the matrix although convergence difficulties sometimes result.

Although the method has so far only been applied to simple elements, the paper has indicated possible techniques for extending the procedure to other elements such as three-dimensional beams and shells that can be formulated using the co-rotational method.

Acknowledgements

The authors would like to thank Dr. Ugo Galvanetto for his contributions to the work with the beam element.

References

1. Stewart, I., 'Warning – Handle with care!', *Nature* **355**, 1992, 16–17.
2. Downer, J. D., Park, K. C., and Chiou, J. C., 'Dynamics of flexible beams for multibody systems: A computational procedure', *Computer Methods in Applied Mechanics and Engineering* **96**, 1992, 373–408.
3. Belytschko, T., 'An overview of semidiscretisation and time integration procedures', in *Computational Methods for Transient Analysis*, T. Belytschko and T. J. R. Hughes (eds.), Elsevier Science, 1983, pp. 1–65.
4. Bathe, K.-J., *Finite Element Procedures in Engineering Analysis*, Prentice-Hall, Englewood Cliffs, 1982.
5. Zienkiewicz, O. C. and Taylor, R. L., *The Finite Element Method*, Vol. 2, fourth edition, McGraw-Hill, London, England, 1991.
6. Crisfield, M. A., *Non-Linear Finite Element Analysis of Solids and Structures*, Vol. 1, Wiley, Chichester, England, 1991.
7. Haug, E., Nguyen, O. S., and De Rouvray, A. L., 'An improved energy conserving implicit time integration algorithm for nonlinear dynamic structural analysis', in *Proceedings of the Fourth Conference on Structural Mechanics in Reactor Technology*, San Francisco, August 1977.
8. Hughes, T. J. R., Liu, W. K., and Caughy, P., 'Transient finite element formulations that preserve energy', *Journal of Applied Mechanics* **45**, 1978, 366–370.
9. Simo, J. C. and Wong, K. K., 'Unconditionally stable algorithms for rigid body dynamics that exactly preserve energy and momentum', *International Journal for Numerical Methods in Engineering* **31**, 1991, 19–52.

10. Simo, J. C., Rifai, M. S., and Fox, D. D., 'On a stress resultant geometrically exact shell model, Part IV: Conserving algorithms for non-linear dynamics', *International Journal for Numerical Methods in Engineering* **34**, 1992, 1117–1164.
11. Hilber, H. M., Hughes, T. J. R., and Taylor, R. L., 'Improved numerical dissipation for time integration algorithms', *Earthquake Engineering and Structural Dynamics* **5**, 1977, 283–292.
12. Zienkiewicz, O. C., Wood, W. L., and Taylor, R. L., 'An alternative single-step algorithm for dynamic problems', *Earthquake Engineering and Structural Dynamics* **8**, 1980, 31–40.
13. Peng, X. and Crisfield, M. A., 'A consistent co-rotational formulation for shells using triangular elements with constant strain and constant curvature', *International Journal for Numerical Methods in Engineering* **35**, 1992, 1829–1847.
14. Crisfield, M. A. and Shi, J., 'A co-rotational element/time integration strategy for non-linear dynamics', *International Journal for Numerical Methods in Engineering* **37**, 1994, 1897–1913.
15. Crisfield, M. A., Shi, J., and Lim, K. L., 'Finite elements and non-linear dynamics', in *Modern Practice in Stress and Vibration Analysis*, The Stress Analysis Group of the Institute of Physics, Sheffield, April 1993, pp. 3–13.
16. Simo, J. C. and Tarnow, N., 'The discrete energy-momentum method. Conserving algorithms for nonlinear elastodynamics', *Zeitschrift für angewandte Mathematik und Physik* **43**, 1992, 757–792.
17. Simo, J. C. and Tarnow, N., 'A new energy conserving algorithm for the nonlinear dynamics of shells', *International Journal for Numerical Methods in Engineering* **37**, 1994, 2527–2549.
18. Bathe, K.-J., *Finite Element Procedures for Solids and Structures – Nonlinear Analysis*, MIT Centre for Advanced Engineering Studies, 1986.
19. Lim, K. L. and Crisfield, M. A., 'Dynamic finite element analysis applied to a simple model exhibiting dynamic instability', *Engineering Computations* **11**, 1994, 483–494.
20. Lim, K. L., 'Dynamic stability of suddenly loaded structures', M.Sc. Thesis, Department of Aeronautics, Imperial College, London, 1992.
21. Oran, C., 'Tangent stiffness in plane frames', in *Proceedings of the American Society of Civil Engineers, Structural Division*, Vol. 99, 1973, pp. 973–985.
22. Crisfield, M. A., 'A consistent co-rotational formulation for non-linear, three-dimensional, beam-elements', *Computational Methods in Applied Mechanics and Engineering* **81**, 1990, 131–150.
23. Rankin, C. C. and Brogan, F. A., 'An element independent corotational procedure for the treatment of large rotations', *ASME, Journal of Pressure Vessel Technology* **108**, 1969, 165–174.